

Nanocomposite Assisted Green Synthesis of Polyvinylpyrrolidone-Silver Nanocomposite Using *Pandanus atrocarpus* Extract for Antiurolithiatic Activity

Abdullah Hasan Jabbar ^{1*}, Hayder Shkhair Obayes AL-Janabi ²,
Maytham Qabel Hamzah ³, Salim Oudah Mezan ⁴, Alaa Nahad Tumah ⁵,
Amira Saryati Binti Ameruddin ⁶, Mohd Arif Agam ⁷

¹⁻⁷ Department of Physics and Chemistry, Faculty of Applied Sciences and Technology, University Tun Hussain Onn Malaysia, Pagoh Campus, Jalan Pancor, 84600 Pancor, Johor, Malaysia

¹ Al-Hussein Teaching Hospital, Directorate of Al-Muthanna Health, Ministry of Health, Republic of Iraq

² Department of Biotechnology, Al-Qasim Green University, Iraq

^{3,4} Directorate of Education Al-Muthanna, Ministry of Education, Republic of Iraq.

E-mail: physics1984@yahoo.com, gw170030@siswa.uthm.edu.my, arif@uthm.edu.my

ABSTRACT

A simple technical which is based on in situ doping of polymers with metal nanocomposite such as Polyvinylpyrrolidone (PVP) with silver nanoparticles (Ag NPs) is elaborated. The fabricate polymer nanocomposites (PVP-Ag NCs) showed altered physical and chemical properties that can be useful in researches involving biological activities. The present study reports an eco-friendly and rapid method for the synthesis of PVP-AgNCs. The PVP-AgNCs is synthesized through a green synthetic method, where *Pandanus atrocarpus* extract was used to act as reducing and capping agent. It is observed that this method is very fast, suitable and the formed PVP-AgNCs took only 5 to 10 min of the reaction time preparation with less energy and non-toxic chemicals. PVP-Ag NCs was characterized by UV-Vis, FESEM, FTIR, and XRD for chemical, morphology and crystallinity behavior of PVP-AgNCs. The unique PVP-AgNCs UV-vis peak is recorded at 450 nm which confirming the synthesis of the nanocomposite. FESEM analysis showed the nanocomposite to be narrow in size ranging from 27 to 50 nm. It is believed that this is the first-ever report on investigating PVP-AgNCs for its antiurolithiatic activity through nucleation assay and dose-dependent. The PVP-Ag NCs powerful bioactivity demonstrated in this report could lead to clinical use as antiurolithiatic agent.

Keywords: Antiurolithiatic; Biological activity; FESEM; Nanocomposite; *Pandanus atrocarpus*.

Correspondence:

Abdullah Hasan Jabbar

Department of Physics and Chemistry, Faculty of Applied Sciences and Technology, University Tun Hussain Onn Malaysia 84600 Pagoh, Malaysia
Al-Hussein Teaching Hospital, Directorate of Al-Muthanna Health, Ministry of Health, Republic of Iraq
physics1984@yahoo.com, gw170030@siswa.uthm.edu.my

INTRODUCTION

The increasing applications of nanomaterials for production of nano-medical related materials and applications have been one of today's major researches. These trend in adopting nanotechnology into medial field is due to unique properties of nanomaterials when materials are reduced to their atomic dimension. Nanomaterials are synthesised from bulk size materials either through the "top-down approach" or from smaller building blocks (bottom-up) (Gayan P. et al., 2015), where reduction in sizes and shapes of these particles allows demonstration of different physical and chemical properties compared to their parent materials (Gentile et al., 2016). The minimization in sizes of materials toward nano dimension, enable penetration of biological nano-dimension materials such as specific molecular and cellular bodies, where the enhancement of the surface area of the nanomaterials

facilitate increasing adsorption for targeted delivery of substances (Singh & Lillard, 2009). Polymer is as host materials for metal nanoparticles attachment or as the nanoparticles embedded in the polymer matrices (Sarkar et al., 2012). A composite material are defined as a mixture made up of materials such as polymers doped with nanoparticles that having strikingly different physical and chemical properties depended to their ratio percentages (Fadiran et al., 2018). The nanocomposites is termed as at least one part of the mixed materials are at nanoscale dimension that sometime enhanced their optical properties (Awad et al., 2012) and ability to be tuned of its physical and chemical properties either by electron beam, laser or gamma irradiation (Adam R. M. et al., 2017).

However, the properties concerning polymer composites rely to the type of nanoparticles (metals, organics or inorganics)

Nanocomposite Assisted Green Synthesis of Polyvinylpyrrolidone–Silver Nanocomposite Using *Pandanus atrocarpus* Extract for Antiurolithiatic Activity

attached or embedded to the polymer that created different new properties when the nanoparticles sizes, shapes, concentrations, or interactions with the polymer matrices (M. A. Agam et al., 2007). Owing to their tuneable properties, polymer nanocomposites such as PVP-AgNCs can be tune of their performance, improved properties compared to their constituent parts, design flexibility, specificity and decrease production costs (Hanemann et al., 2010). The nanocomposite can consist of organic (host polymers)/inorganic and organic/organic nanoparticles where the host polymers they are found applicable as catalysis, bioengineering, photonics, electronics, and antibacterial activities (Gu et al., 2015). AgNPs have long favoured to form composites with polymers, such as with polyvinyl alcohol, polypyrrole, polyvinylidene fluoride, chitosan, and cellulose. The main problem in synthesizing silver-polymer nanocomposite, is the homogenous distribution of Ag nanoparticles (Muhammad I. S. et al., 2019; A. Hasan J. et al., 2018). The homogenous distribution of the silver nanoparticles in the polymer matrices can be addressed through in-situ polymerization technique. These polymer-silver nanocomposites may have a broad range applications such as in biomedicine, textiles, cloud treatment, food storage containers, domestic appliances, or medical devices (Sadasiivuni et al., 2019).

Urolithiasis is the condition where urinary calculi are formed or located anywhere in the urinary system or the process of formation of stone in kidney, bladder or ureter (Kifayatullah et al., 2019). It is considered as the third most common affliction of the urinary tract (Marcon et al., 2019). The major part of the population and the medical experts are trying to find alternatives medical treatment, as many modern drugs have some form of side effects (Patle et al., 2019), which is said to be better approach using nanotechnology advancement in medical (Jeevanandam et al., 2018). Therefore, the present study focuses on the synthesis and characterization of nanosize PVP-AgNCs, where Ag nanoparticles were synthesis from *pandanus atrocarpus* extract as Ag reduction agent and later investigated its biomedical properties as antiurolithiatic activity. It is vital to find alternative technique, such as PVP-AgNCs as antiurolithiatic agent in the attempt to apply nanotechnology advancement as new approach for future medical treatment (Zhu et al., 2007).

MATERIALS AND METHODS

Preparation of *Pandanus atrocarpus* aqueous extract

Pandanus atrocarpus (PA) plant was supplied by Ethno Resources Sdn. Bhd. (Selangor, Malaysia). The plant sample was stored at 4 °C until further use. The protocol described by (Awad et al., 2019) was used for the preparation of aqueous extract. In brief, 2 g of PA whole plant powder was boiled in 100 mL distilled water. The filtered extract was in concentrated form and let too dry in a hot air oven at 40 °C for 48 hours to obtain a dark brown semisolid mass which was weighed and labelled as PAE. The PAE was stored at 4 °C and used for further experiments.

Synthesis of AgNPs

Synthesis of the silver nanoparticles is through PAE (0.8 ml added to the AgNO₃ solution and the volume was adjusted to 10 ml with de-ionized water (Xu, X, et al., 2017). The final concentration of Ag⁺ was 1 × 10⁻³ M. The solution was stirred for 2 min. The reduction process Ag⁺ to Ag⁰ nanoparticles was followed by the color change of the solution from yellow to brownish-yellow to deep brown depending on parameters studied such as the extract concentration, temperature and pH. The nanoparticles were prepared at different pH values, the pH of the solutions was adjusted using 0.1 NH₃PO₄ or 0.1 N NaOH solutions (Khalil et al., 2014).

Synthesis of PVP/Ag Nanocomposite

PVP-AgNC synthesized by the method of (Awad et al. 2015) with slight modifications. PVP dissolve with distilled water (DW) for prepare a 20 % stock solutions. The synthesized PAE-AgNPs (Previous section) mixed with of PVP (40%) in different ratios (1:9, 2:8, 3:7, 4:6, 5:5, 6:4, 7:3, 8:2 and 9:1) The resulting reaction mixture monitored for change in color visually as well as by recording UV-vis spectra at regular intervals within the wavelength range of 300 to 700 nm. PVP-Ag nanocomposite has further characterized.

Characterization of Ag NPs and PVP-Ag NCs

The synthesis of Ag NPs and PVP-Ag NCs was confirmed by periodically scanning the absorption maxima of aliquots (1.0 mL) of the reaction solution in 1-cm path-length disposable cuvettes. The UV-vis spectra was recorded every 30 minutes within the wavelength of 300 to 700 nm (Ahmed et al., 2016). The possible biomolecules of PAE responsible for bio reduction of silver ions were identified by recording the Fourier transform infrared (FTIR) spectrum of Ag NPs using Perkin Elmer Spectrum FTIR in the range of 4000–450 cm⁻¹ at a resolution of 4 cm⁻¹ (Ovais et al., 2016). The powder AgNPs sample used for X-ray diffraction measurements performed on Shimadzu XRD 6000 diffractometer operating at 40 kV in the region of 2θ from 30° to 80° at a speed of 0.02°/min (Ali et al., 2016). For size and shape analysis of AgNPs, the field emission scanning electron microscope (FESEM) images were captured on JEOL JSM-7600F at an accelerating voltage of 10 keV. The size analysis from FESEM images was performed on image 1.52 g software (Mohseni et al., 2019).

Antiurolithiatic Activity

Nucleation Assay

The inhibitory activity of the test drugs on initiation of CaOx crystallization (nucleation rate) in the absence or presence of inhibitors was performed according to (Zaki et al., 2019) method. Briefly, both solutions of calcium chloride (5 mmol/l) and sodium oxalate (7.5 mmol/l) were prepared in a buffer containing 0.05 mol/l Tris-HCl and 0.15 mol/l NaCl at pH range of 6.5. An aliquot of calcium chloride (950 µl) was mixed with 100 to 500 µl of PVP-AgNCs and PAE. The crystallizations was start by the added 950 µl from sodium oxalate (7.5 mmol/l) at 37°C. The optical density of the reaction mixture was monitored at 620 nm using UV-visible

spectrophotometer over 10 min. All the experiments were performed in triplicate and the rate of nucleation was determined by comparing the induction time of crystals in the absence (control) or presence of the test drugs. The percentage of inhibition was calculated by following formula:

$$\% \text{ nucleation inhibition} = [(\Delta A \text{ control} - \Delta A \text{ test}) / \Delta A \text{ control}] \times 100$$

RESULTS AND DISCUSSION

Uv-Vis (Ultraviolet-visible Spectroscopy)

The formation of PVP-AgNCs were confirmed by UV-Vis spectral study. The synthesis of AgNPs were first as yellowish in colour, the colour of AgNO₃, that later turned to green as PA extract was mixed in AgNO₃ solution. When the Silver (Ag) is reduced by the biological process of PA, the solution turned to brown indicating the formation of AgNPs and confirmed by UV-Vis spectroscopy (Edison et al., 2017). The solution colour changes from yellowish to green and later to brown, are simple indication of the reduction of silver metal particles Ag⁺ to AgNPs. This colour refers to the unrest on Surface Plasmon Resonance (SPR). As shown in Figure 1, the attributed of SPR spectrum of AgNPs and when it is in composite, PVP-AgNCs showed peaks around 432 nm and 420 nm, respectively indicating the AgNPs are formed and absorbing waves uniquely.

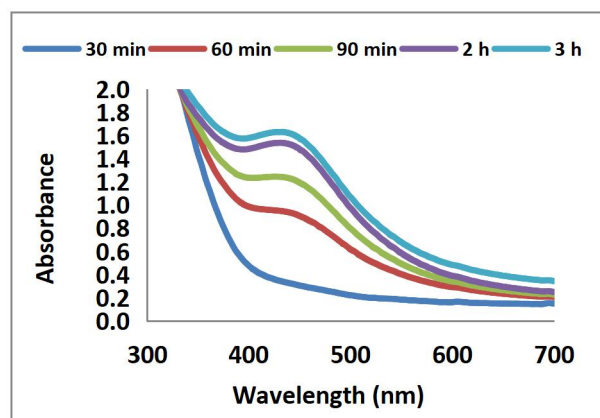


Figure 1: UV-VIS absorbance spectra for various weight-of (wt %) AgNO₃ and different concentrations

Fourier Transformed Infrared Spectrometry (FTIR)

The prominent peaks present in PAE are located at 3338, 2131, 1638, 1295, and 428 as shown in Fig. 2. It may be inferred from Fig. 2 that the peaks shift of the PVP-AgNCs with varying concentration AgNO₃ do not considerably differ from each other as all the five spectres are found very closely overlapped. In all of the PVP-AgNCs samples, the same two peak shifts after AgNPs synthesis were observed as: 3290 to 3270/3310 cm⁻¹ and 1636 to 1637/1639 cm⁻¹, as recorded for AgNPs samples 1 to 5. The peak at 3338 belongs to the -OH group which, in this case, can be attributed to the phenolic and flavonoid compounds of PAE. Second important stretching vibration is recorded from 1636 to 1636/1635 cm⁻¹ which, although may be considered as amide group of proteins as well as benzene ring containing aromatic compounds, it may also be taken into account for phenolic and flavonoid compounds as they exhibit strong vibration on

this wavenumber (Shivakumar et al., 2014; Prathna et al., 2011). In the context of all these stretching vibrations found in the FTIR spectra of PAE-AgNCs, it may be assumed that they have played a role in accelerating the rate of AgNPs synthesis reaction leading to the nucleation along with stalling the secondary growth of the nuclei.

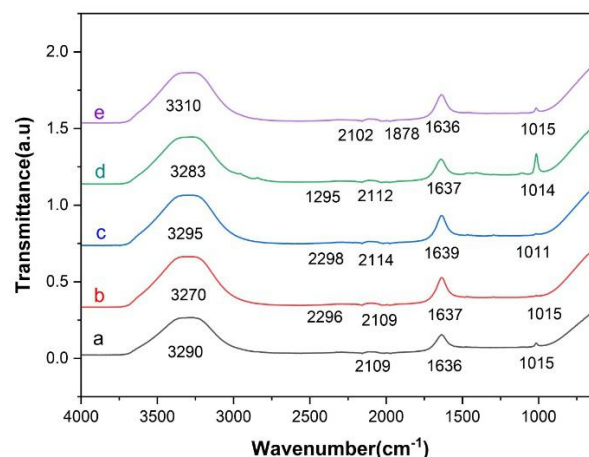


Figure 2: FTIR spectra for irradiated Ag/ PVP NCs at (a) (10 PVP-Ag) (b) (20 PVP-Ag) (c) (30 PVP-Ag) (d) (40 PVP-Ag) (e) (50 PVP-Ag).

Field Emission Scanning Electron Microscopy (FESEM)

The particle sizes and morphology analysis were performed by Field Emission Scanning Electron Microscope (FESEM). The FESEM micrographs of the AgNPs and PVP-AgNCs are mostly taken at the magnification of 200,000× as shown in Figure 3. The shape of the PVP-AgNCs are almost spherical and the smallest particle found is about 19.57 nm. The function of PVP in the PVP-AgNCs is not only as a binder, but it also prevents the process of agglomeration of Ag nanoparticles and limits the diameter of the nanoparticles formed (Zhang et al., 2011; Flahaut et al., 2000). As for the morphology of particles in nanocomposite, it is evident that the particles obtained in this study are mostly spherical in shape.

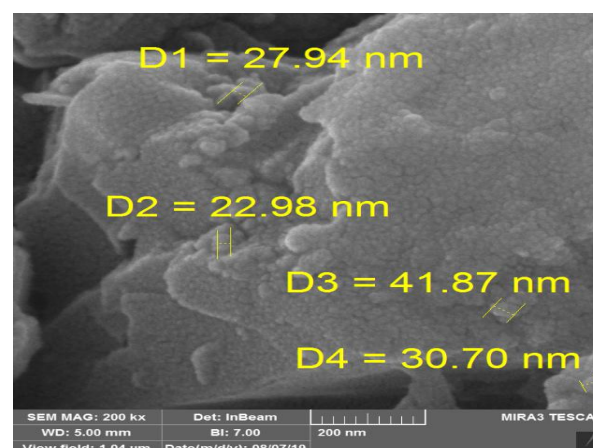


Figure 3: Microstructure concerning the conductive film FESEM

XRD (X-ray Diffraction)

Nanocomposite Assisted Green Synthesis of Polyvinylpyrrolidone-Silver Nanocomposite Using *Pandanus atroparpus* Extract for Antiuro lithiatic Activity

The XRD analysis of PVP/AgNCs were carried out to confirm the crystalline nature of the synthesized nanomaterials. Figure 4 shows XRD spectrum of AgNPs and PVP/AgNCs, respectively. The X-ray diffractograms, at 2θ from 20° - 80° , clearly indicate the crystallinity of the tested samples as indicated by the broadening of Bragg's peaks. The presence of sharp peaks indicates the bioactive compounds present on the surface of the NPs (Shabestarian et al., 2017). The Bragg's reflection values of 38° , 44° , 64° and 77° , obtained for AgNPs and PVP/AgNC, corresponding to the set of lattice planes, that is, (111), (200), (220) and (311) have been obtained at 2θ indicating the formation of face centred cubic (fcc) crystalline structure of silver nanostructure. The peak related to the lattice plane (111) is the most intense suggesting its most predominant orientation in addition to the crystalline nature of the synthesized silver colloids. The XRD spectrum did not show any other crystallographic peaks confirming the high purity of synthesized Ag colloids. Similar results have been reported recently for the synthesis of AgNPs-mediated nanocomposite (Awad et al., 2015).

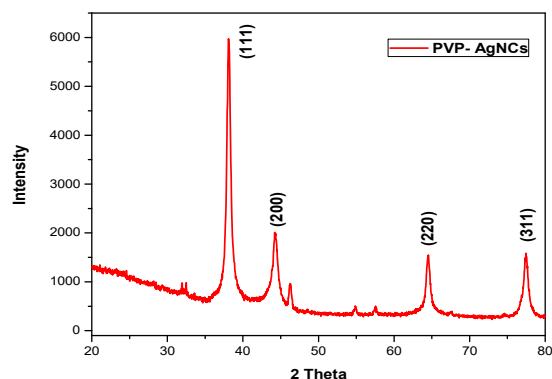


Figure 4: XRD pattern of PVP/AgNC

Table 1: XRD Peaks list of PVP/Ag NCs

Pos. [2θ .]	Height [cts]	FWHM Left [2θ .]	d-spacing [\AA]	Rel. Int. [%]
38.0589	4981.03	0.4428	2.36445	10.00
44.2253	1324.48	0.4723	2.04803	26.59
64.5287	1127.84	0.2066	1.44417	22.64
77.4782	1191.13	0.4723	1.23197	23.91

Determination of Antiuro lithiatic Activity

The formation of renal stones in the urinary tract is mostly attributed to the supersaturation of calcium oxalate, the most common part of kidney stones, leading to the particle crystallization in the urinary tract with nucleation, growth, and aggregation being the subsequent steps. As the particle crystallization is one of the initial steps in the process of renal stone formation, the current research was focused on

the investigation of antiuro lithiatic potential of AgNPs and PVP-AgNCs in terms of the inhibition of crystallization of calcium oxalate.

The increase in turbidity in response to the inhibition of calcium oxalate crystallization by phytochemicals is considered as the basic parameter of spectrophotometric antiuro lithiatic assays. Tables 2 shows the crystallization inhibition by AgNPs and PVP-AgNCs samples in terms of the absorbance values with respect to control as recorded by time-course measurement.

Table 2: In vitro inhibition of calcium oxalate crystallization

Time (min)	Control	SD (\pm)	Cystone	SD (\pm)	PVP-AgNC	SD (\pm)
2	0.0735	0.006364	0.0335	0.006364	0.0240	0.005657
4	0.1520	0.001414	0.0310	0.002828	0.0480	0.007071
6	0.2295	0.003536	0.0580	0.005657	0.1130	0.001414
8	0.2715	0.003536	0.0715	0.003536	0.1725	0.002121
10	0.3365	0.003536	0.1065	0.003536	0.1965	0.003536
12	0.3920	0.004243	0.1395	0.007778	0.2570	0.002828
14	0.4370	0.002828	0.1535	0.007778	0.2940	0.007071
16	0.4490	0.005657	0.1590	0.005657	0.2995	0.004950

Fig. 5 shows the antiuro lithiatic activity of AgNPs and PVP-AgNCs samples in terms of crystallization inhibition of calcium oxalate as shown by a decrease in absorbance with respect to the control (the reaction mixture without AgNPs or PVP-AgNCs). It is clear that all the AgNPs and PVP-AgNCs samples inhibited calcium oxalate crystallization in artificial urine. However, AgNPs showed the more antiuro lithiatic activity by inhibiting calcium oxalate crystallization as compared to the PVP-AgNCs. At the maximum volume concentration of $500 \mu\text{L}$, the absorbance values of AgNPs and PVP-AgNCs at 16 min in calcium oxalate crystallization assay were recorded at 0.2345 and 0.2995, respectively, which are significantly different ($p < 0.05$) from that of the control recorded at 0.4490.

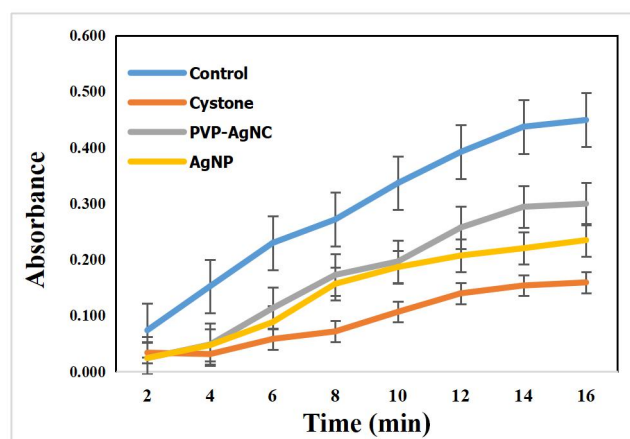


Figure 5: Calcium oxalate crystallization assay with respect to time-course measurement of absorbance.

Literature review did not produce a single research reported on antiurolithiatic activity of PAE-mediated AgNPs, PVP-Ag NCs. The literature search with various combinations of the keywords “in vitro antiurolithiatic”, “in vitro antilithiatic”, “*Pandanus atropicus*”, PVP-Ag NCs and Ag NPs revealed no research papers in PubMed and PPA databases. However, there are many research reports in the literature that have described in vivo and vitro antiurolithiatic effect on various plant extracts and indicated the link between polyphenolic phytochemicals and antiurolithiatic activity. Saha et al. used the classic model of artificial urine to determine the antiurolithiatic effect *B. ciliata* (*Bergiana ciliata*) extract and reported that the polyphenolic compounds, especially the saponins in the extract, inhibited the in vitro calcium oxalate crystallization. Pawar et al. induced urolithiasis in rats by surgical implants of zinc disc in the urinary bladder and studied the antiurolithiatic effect of methanolic and chloroform extracts of *Abelmoschus moschatus* seeds at various doses. They reported methanolic extract at all doses whereas chloroform extract at higher doses only inhibited the growth of calculi.

Devkar et al. evaluated the antiurolithiatic activity of different solvent extracts of *Lepidagathis prostrata* (all reported to contain polyphenolic compounds) by using in vitro calcium oxalate nucleation and aggregation assays and reported that ethyl acetate extract showed the highest inhibition of nucleation and aggregation recorded at IC₅₀ (inhibitory concentration) of 336.23 ± 30.79 and 149.63 ± 10.31 µg/mL, respectively. The in vitro antilithiatic activity of hydroalcoholic extract of *Cinnamomum zeylanicum* was examined in a metastable solution of calcium chloride and sodium oxalate by (Zaki et al. 2019) who reported that the crystal nucleation was significantly reduced (p < 0.001) at 4, 8 and 10 mg/mL concentration of extract with maximum inhibition of 92.46 % at 2 mg/mL. They also reported that the maximum aggregation inhibition of 100 % was found at 410 mg/mL extract concentration. The authors ascribed the antiurolithiatic activity of *Cinnamomum zeylanicum* to saponins, the phenolic compounds, in addition to many other phytochemicals present in the extract. Similar observation related to the antiurolithiatic activity of the standardized extract of *Biophytum sensitivum* was reported by (Pawar et al., 2015), who also revealed the presence of polyphenolic

compounds in the extracts in the phytochemical analysis. (Siddiqui et al. 2018) evaluated the in vivo and in vitro antiurolithiatic effect of *Citrullus lanatus*. They reported that the pulp extract of *Citrullus lanatus* reduced the calcium oxalate crystallization in the in vivo male Wistar rat model of urolithiasis in addition to the inhibition of in vitro crystallization in supersaturated solution of calcium and oxalate.

The results of this study show that AgNPs and PVP-AgNCs possess good CaOx crystallization inhibition activity. The antiurolithiatic activity of these samples may be attributed to the polyphenolic compounds capping and stabilizing the nanoparticles. Table 3 shows In-vitro inhibition of calcium oxalate crystallization and PVP-AgNCs that is close to Cystone inhibition, while figure 6 shows comparison in percentages of inhibition.

Table 3: In-vitro inhibition of calcium oxalate crystallization

Concentration µL	AgNPs± SD	PVP- AgNCs ±SD	Cystone ± SD
100	50±1	54±2.0	75±1
200	55±1.5	69±1.0	78±1
300	59±0.7	76±1.0	70±1
400	63±1	78±0.5	84±1
500	71±1.2	80±0.8	87±1

The antiurolithiatic activity may be attributed to the polyphenolic compounds present in the tested extracts as revealed by the phytochemical analysis of both AgNPs and PVP-AgNCs. In Figure 6 shows the percentage of inhibitory that PVP-AgNCs are so much similar inhibitor compared to Cystone. Figure 7 compared the concentration effects where the concentration of 100 µL is found to be giving better antiurolithiatic activity, nevertheless the graph could be broadly diverted for much longer period of duration. These results indicated at lower time the antiurolithiatic is corresponded to the present of nanoparticles much more than concentration, where at longer duration, the antiurolithiatic will be influenced more by concentration. Higher concentration will have less active surfaces compared to lower concentration beside the AgNPs could be agglomerated due to higher concentration.

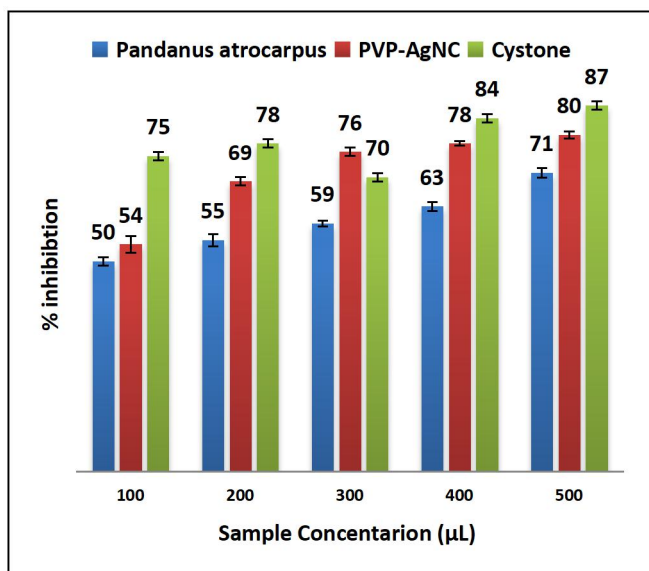


Figure 6: CaOx crystallization inhibition assay for PAE, AgNPs, and PVP-AgNCs.

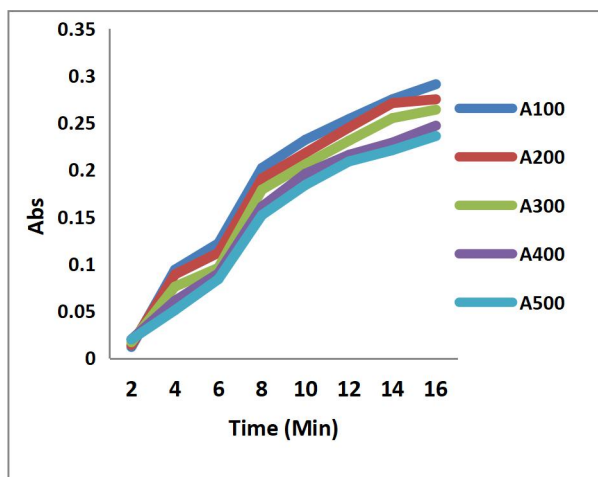


Figure 7: The antiuro lithiatic activity with different concentrations

CONCLUSION

Nanobiotechnology represents a new era of innovative approach to develop and test modern drug formulations based on biosynthesized nanoparticles and nanocomposites with different biological activities such as antimicrobial, antioxidant and anticancer properties. Physical characteristics of silver nanoparticles and nanocomposites, such as shape and size, are important for augmenting antiuro lithiatic activity. The biosynthesized silver PVP-AgNCs using *P. atrocarpus* aqueous extract demonstrated excellent antiuro lithiatic activity. Silver nanoparticles might be useful for the development of newer and more potent antiuro lithiatic agents. The data represented in our study contribute to a novel and unexplored area of nano-materials as alternative medicine. Therefore, further studies are needed to fully characterize the mechanisms involved with the antiuro lithiatic activity of these particles.

ACKNOWLEDGMENT

This work was funded by the Fundamental Research Grant awarded by the Ministry of Higher Education Malaysia, [FRGS/1/2019/STG07/UTHM/02/5 (FRGS K171)] and TIER 1 (H218) and GPPS (H423), awarded by University Tun Hussein Onn (UTHM), Malaysia.

CONFLICT OF INTEREST: The authors have no conflicts of interest to declare

REFERENCES

- Ahmed, S., Saifullah, Ahmad, M., Swami, B. L., & Ikram, S. (2016). Green synthesis of silver nanoparticles using *Azadirachta indica* aqueous leaf extract. *Journal of Radiation Research and Applied Sciences*, 9(1), 1-7.
- Adam R. M. A, Jibrin A. Y, Mohamad F. B. H, Y. S. K, Mohammed I. K, Muhammad N. M, Mohd A. A. (2017). Synthesis and microwave absorption properties of doped expanded polystyrene with silver nanoparticles, 3rd International Conference on the Application of Science and Mathematics, SCIE MATHIC, 9, (3), p. 33-40
- Ali, M., Kim, B., Belfield, K. D., Norman, D., Brennan, M., & Ali, G. S. (2016). Green synthesis and characterization of silver nanoparticles using *Artemisia absinthium* aqueous extract—a comprehensive study. *Materials Science and Engineering: C*, 58, 359-365.
- Awad, M. A., Hendi, A. A., Ortashi, K. M., Alanazi, A. B., ALZahrani, B. A., & Soliman, D. A. (2019). Greener Synthesis, Characterization, and Antimicrobial Effects of Helba Silver Nanoparticle-PMMA Nanocomposite. *International Journal of Polymer Science*, 2019.
- Awad, M. A. W. K. Mekhamer, N. M. Merghani et al., “Green synthesis, characterization, and antibacterial activity of silver/- polystyrene nanocomposite,” *Journal of Nanomaterials*, vol. 2015, Article ID 943821, 6 pages, 2015.
- Das, D., Nath, B. C., Phukon, P., & Dolui, S. K. (2013). Synthesis of ZnO nanoparticles and evaluation of antioxidant and cytotoxic activity. *Colloids and Surfaces B: Biointerfaces*, 111, 556-560.
- Devkar, R. A., Chaudhary, S., Adepu, S., Xavier, S. K., Chandrashekar, K. S., & Setty, M. M. (2016). Evaluation of antiuro lithiatic and antioxidant potential of *Lepidagathis prostrata*: A Pashanbhed plant. *Pharmaceutical biology*, 54(7), 1237-1245.
- Edison, T. N. J. I. & Sethuraman, M. G. (2017). Areca catechu Assisted Synthesis of Silver Nanoparticles and its Electrocatalytic Activity on Glucose Oxidation. *J Clust Sci*, DOI 10.1007/s10876-017-1284.
- Fadiran OO, Girouard N, Meredith JC (2018) Pollen fillers for reinforcing and strengthening of epoxy composites. *Emergent Mater* 1(1–2):95–103
- Flahaut E, Peigney A, Laurent C, Marliere C, Chastel F, Rousset A. Carbon nanotube–metal– oxide nanocomposites: microstructure, electrical conductivity and mechanical properties. *Acta Materialia*. 2000;48(14):3803-12.
- Gayan P., Nilwala K., Atula S., Ajith de A., V. K., (2015). Synthesis of Magnetite Nanoparticles by Top-Down Approach from a High Purity Ore., *Journal of Nanomaterials*, ID 317312, 8 pages <http://dx.doi.org/10.1155/2015/317312>.

12. A. H. J, Maytham Q. H, Salim O. M, Amira S. Binti A, Mohd Arif Agam, (2018), Green Synthesis of Silver/Polystyrene Nano Composite (Ag/PS NCs) via Plant Extracts Beginning a New Era in Drug Delivery, *Indian Journal of Science and Technology*, 11(22), 1-9.
13. Gentile, A., Ruffino, F., & Grimaldi, M. G. (2016). Complex-morphology metal-based nanostructures: fabrication, characterization, and applications. *Nanomaterials*, 6(6), 110.
14. Hanemann, T., & Szabó, D. V. (2010). Polymer-nanoparticle composites: from synthesis to modern applications. *Materials*, 3(6), 3468-3517.
15. Jeevanandam, J., Barhoum, A., Chan, Y. S., Dufresne, A., & Danquah, M. K. (2018). Review on nanoparticles and nanostructured materials: history, sources, toxicity and regulations. *Beilstein journal of nanotechnology*, 9(1), 1050-1074.
16. Khalil, M. M., Ismail, E. H., El-Baghdady, K. Z., & Mohamed, D. (2014). Green synthesis of silver nanoparticles using olive leaf extract and its antibacterial activity. *Arabian Journal of Chemistry*, 7(6), 1131-1139.
17. Kifayatullah, M., Rahim, H., Jan, N. U., Abbas, S., Khan, M. S., & Ikram, M. (2019). Anti-Urolithiatic Effect of *Pericampylus glaucus* against Ethylene Glycol Induced Urolithiasis in Male Sprague Dawley Rats. *Sains Malaysiana*, 48(5), 1075-1081.
18. Marcon, J., Schubert, S., Stief, C. G., & Magistro, G. (2019). In vitro efficacy of phytotherapeutics suggested for prevention and therapy of urinary tract infections. *Infection*, 1-8.
19. M. A. Agam, Q. Guo, (2007), Electron Beam Modification of Polymer Nanospheres, *Journal of Nanoscience and Nanotechnology* Vol.7, 1-5
20. Muhammad M., Ishaq A. G, Mohammed A. A, Hazel M. M-Peraltab, Nadiah K, Jibrin A. Y, Muhammad I. K. BIOSORPTION OF HEAVY METALS BY SCENEDESMUS SP. ISOLATED FROM THE TEMPORARY WATERS OF ENDAU ROMPIN, JOHOR, MALAYSIA, *Jurnal Teknologi*, 77 (24) 35–38
21. Ovais, M., Khalil, A. T., Raza, A., Khan, M. A., Ahmad, I., Islam, N. U. & Shinwari, Z. K. (2016). Green synthesis of silver nanoparticles via plant extracts: beginning a new era in cancer theranostics. *Nanomedicine*, 12(23), 3157-3177.
22. Patle, A., Hatware, K. V., Patil, K., Sharma, S., & Gupta, G. (2019). Role of Herbal Medicine in the Management of Urolithiasis—A Review for Future Perspectives. *Journal of Environmental Pathology, Toxicology and Oncology*, 38(2).
23. Pawar, A. T., & Vyawahare, N. S. (2015). Anti-urolithiatic activity of standardized extract of *Biophytum sensitivum* against zinc disc implantation induced urolithiasis in rats. *Journal of advanced pharmaceutical technology & research*, 6(4), 176.
24. Prathna, T.; Chandrasekaran, N.; Raichur, A.M.; Mukherjee, A. (2011). Biomimetic synthesis of silver nanoparticles by Citrus limon (lemon) aqueous extract and theoretical prediction of particle size. *Colloids Surf. B Biointerfaces*, 82, 152–159.
25. Sadasivuni, K. K., Rattan, S., Waseem, S., Brahme, S. K., Kondawar, S. B., Ghosh, S., ... & Mazumdar, P. (2019). Silver Nanoparticles and Its Polymer Nanocomposites—Synthesis, Optimization, Biomedical Usage, and Its Various Applications. In *Polymer Nanocomposites in Biomedical Engineering* (pp. 331-373). Springer, Cham.
26. Saha, S., & Verma, R. J. (2013). Inhibition of calcium oxalate crystallisation in vitro by an extract of *Bergenia ciliata*. *Arab journal of urology*, 11(2), 187-192.
27. Sarkar, S., Guibal, E., Quignard, F., & SenGupta, A. K. (2012). Polymer-supported metals and metal oxide nanoparticles: synthesis, characterization, and applications. *Journal of Nanoparticle Research*, 14(2), 715.
28. Shabestarian, H., Homayouni-Tabrizi, M., Soltani, M., Namvar, F., Azizi, S., Mohamad, R., & Shabestarian, H. (2017). Green synthesis of gold nanoparticles using Sumac aqueous extract and their antioxidant activity. *Materials Research*, 20(1), 264-270.
29. Siddiqui, W. A., Shahzad, M., Shabbir, A., & Ahmad, A. (2018). Evaluation of anti-urolithiatic and diuretic activities of watermelon (*Citrullus lanatus*) using in vivo and in vitro experiments. *Biomedicine & Pharmacotherapy*, 97, 1212-1221.
30. Pawar, A. T., & Vyawahare, N. S. (2016). Antiurolithiatic activity of *Abelmoschus moschatus* seed extracts against zinc disc implantation-induced urolithiasis in rats. *Journal of basic and clinical pharmacy*, 7(2), 32.
31. Shivakumar S. P. & Vidyasagar G. M. (2014). Biosynthesis, characterization, and antidermatophytic activity of silver nanoparticles using Raamphal plant (*Annona reticulata*) aqueous leaves extract. *Indian J Mater Sci*, 2014; 1-5.
32. Singh, R., & Lillard Jr, J. W. (2009). Nanoparticle-based targeted drug delivery. *Experimental and molecular pathology*, 86(3), 215-223.
33. Xu, X., Yu, T., Bi, Z., Ma, W., Li, Y., & Peng, Q. (2017). Realizing Over 13% Efficiency in Green-Solvent-Processed Nonfullerene Organic Solar Cells Enabled by 1,3,4-Thiadiazole-Based Wide-Bandgap Copolymers. *Advanced Materials*, 30(3), 1703973. doi:10.1002/adma.201703973
34. Zaki, S., Jahan, N., Kalim, M., & Islam, G. (2019). In vitro antilithiatic activity of the hydro-alcoholic extract of *Cinnamomum zeylanicum* Blume bark on calcium oxalate crystallization. *Journal of integrative medicine*.
35. Zhang J, Xiong Z, Zhao X. Graphene–metal–oxide composites for the degradation of dyes under visible light irradiation. *Journal of Materials Chemistry*. 2011;21(11):3634-40.
36. Zhu C-L, Chou S-W, He S-F, Liao W-N, Chen C-C. Synthesis of core/shell metal oxide/polyaniline nanocomposites and hollow polyaniline capsules. *Nanotechnology*. 2007;18(27):275604